Title

Dimethylmercury as a Source of Monomethylmercury in a Highly Productive Upwelling System.

Journal

Environmental Science & Technology, 58(24)

Authors

Adams, Hannah

Cui, Xinyun

Lamborg, Carl

et al.

Publication Date

2024-06-18

DOI

10.1021/acs.est.4c01112

Peer reviewed

Environmental Science & Technology

Editors' Choice
Open Access

pubs.acs.org/est

Article

Dimethylmercury as a Source of Monomethylmercury in a Highly Productive Upwelling System

Hannah M. Adams,* Xinyun Cui, Carl H. Lamborg, and Amina T. Schartup*

Cite This: *Environ. Sci. Technol.* 2024, 58, 10591−10600

Read Online

ACCESS | Metrics & More | Article Recommendations | Supporting Information

ABSTRACT: Monomethylmercury (MMHg) is a neurotoxicant that biomagnifies in marine food webs, reaching high concentrations in apex predators. To predict changes in oceanic MMHg concentrations, it is important to quantify the sources and sinks of MMHg. Here, we study mercury speciation in the California Current System through cruise sampling and modeling. Previous work in the California Current System has found that upwelling transports mercury-enriched deep waters to productive surface waters. These upwelled waters originate within the California Undercurrent water mass and are subsequently advected as a surface water parcel to the California Current. Between the two major water masses, we find that compared to the California Current, the California Undercurrent contains elevated dissolved total mercury (THg) and dimethylmercury (DMHg) concentrations by 59 and 69%, respectively. We explain that these differences result from losses during advection, specifically scavenging of THg and DMHg demethylation. We calculate a net DMHg demethylation rate of 2.0 ± 1.1% d^{-1} and build an empirically constrained mass budget model to demonstrate that net DMHg demethylation accounts for 61% of surface MMHg sources. These findings illustrate that DMHg is a significant source of MMHg in this region, challenging the current understanding of the major sources of marine MMHg.

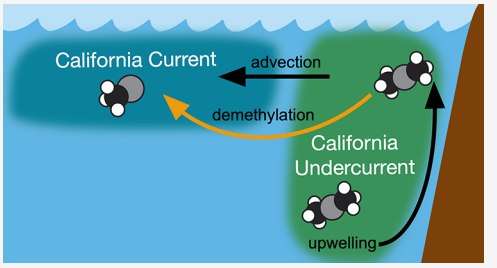

KEYWORDS: *California Current, mercury biogeochemistry*

INTRODUCTION

Monomethylmercury (MMHg) is a neurotoxicant of global concern that biomagnifies in marine food webs.[1] Humans are predominately exposed to MMHg through the consumption of seafood. The California Current System (CCS) is a highly productive fishery accounting for 0.5 billion dollars in seafood revenue in 2019.[2] This fishery is supported by seasonal upwelling of nutrient-enriched deeper waters to the surface that sustain biological activity primarily in the spring and summer.[3]

One potential source of MMHg is dimethylmercury (DMHg) demethylation, and previous research in the CCS focused on the impact of upwelling on mercury (Hg) speciation, specifically DMHg. In 2009, Conaway et al. measured high DMHg concentrations during the upwelling season, and they proposed that microbial degradation associated with remineralization favors DMHg production.[4] Years later, Coale et al. measured elevated DMHg concentrations in upwelling mesoscale eddies throughout the CCS.[5] These studies concluded that upwelling impacts the upper water column total Hg (THg) and DMHg concentrations by transporting Hg-enriched deep waters to the surface, but they did not address how DMHg demethylation impacts MMHg concentrations within the water column.

Here, we propose that the demethylation of upwelled DMHg is a major source of surface MMHg in the CCS. We followed two surface water parcels and sampled a transect to investigate Hg speciation within the major water masses of the region. Typically, upwelled waters originate within the California Undercurrent water mass[6] and are advected to the California Current water mass over the course of 40−80 days.[7] Collecting and analyzing samples during water parcel advection allowed us to compare these two water masses to create a "natural laboratory" to quantify rates for *in situ* Hg biogeochemical transformations. These rates can then be incorporated into a regional mass balance model to evaluate the major sources and sinks for each Hg species.

Within a water mass, THg concentrations reflect the balance of the sources and sinks of Hg. Removal of dissolved THg can occur through scavenging of inorganic divalent Hg (Hg^{II}) and MMHg or evasion of elemental Hg (Hg^0) and DMHg.[5,8,9] Hg^{II} is considered the main substrate for MMHg production,[10,11] and MMHg formation is enhanced in oxygen minimum zones globally[12−15] due to its production by anaerobic or microaerophilic microbes in water and on particles.[16−20] While it is unclear how DMHg is formed in the ocean, one study reported DMHg formation from both Hg^{II} and MMHg in unfiltered

Received: January 30, 2024
Revised: May 7, 2024
Accepted: May 8, 2024
Published: June 7, 2024

https://doi.org/10.1021/acs.est.4c01112
Environ. Sci. Technol. 2024, 58, 10591−10600

seawater,[21] and a laboratory experiment showed DMHg formation from MMHg on reduced sulfide mineral surfaces.[22] Elevated DMHg concentrations found in the Peruvian Upwelling System oxygen minimum zone[13] suggest that low oxygen conditions favor both DMHg and MMHg formation. Within the California Undercurrent, remineralization fueled by surface productivity depletes oxygen concentrations below 100 m depth.[23,24] These conditions of high particle and low oxygen concentrations within the California Undercurrent could be favorable for the formation of MMHg and DMHg at depth.

With seasonal upwelling, MMHg and DMHg are transported to the surface from depth and can convert into Hg^{II} and MMHg through photodemethylation and biological (or dark) demethylation.[20,25−30] MMHg demethylation has been studied globally to determine rates through field incubation experiments.[15,20,26−31] Conversely, DMHg demethylation to MMHg has only been studied in the laboratory,[25,32] and these rates have not been measured in the field. Environmentally representative Hg transformation rates are necessary for global biogeochemical models to predict the balance of Hg speciation within the ocean, and current models can be improved by incorporating region-specific DMHg formation and degradation rates.[33,34] Thus, expanding global DMHg measurements and studying DMHg formation and degradation mechanisms *in situ* are essential to effectively quantify the sources of MMHg.

To quantify the contribution of DMHg demethylation to the MMHg pool in surface (<200 m) waters, we measured dissolved THg, MMHg, Hg^0, and DMHg concentrations in 16 profiles and 12 benthic boundary layer (BBL) samples during the 2021 California Current Ecosystem Long-Term Ecological Research (CCE LTER) Process Cruise. We analyzed changes in Hg speciation between the two major water masses of the CCS, and we constructed an empirically constrained mass budget and used it to model the sources of MMHg in surface waters in the region.

METHODS

Sampling Plan. This study was conducted during the CCE LTER P2107 Process Cruise from July 10th to August 8th, 2021, on board the *R/V Revelle*, where we sampled two water parcels and a seven station transect. Water parcels were sampled during a Lagrangian-style process study using drifter floats modeled after previous CCE LTER cruises.[35,36] During these process studies, an upwelled water parcel from the California Undercurrent water mass was identified by satellite temperature and chlorophyll-*a* (chl-*a*) concentrations. We followed the upwelled water parcel for 11 days and a water parcel at the eastern edge of the oligotrophic gyre for 3 days (Figure 1). Profiles for dissolved Hg concentrations, including THg, DMHg, MMHg, and Hg^0, were taken every other day during the process studies. A seven station transect from stations S1−S7 was conducted across the California Current water mass, and profiles for THg, DMHg, and Hg^0 were taken for all stations in the transect. A MMHg profile was taken only for Station S4 in the transect. Stations are colored based on their corresponding water mass in Figure 1, and water masses are categorized by the temperature−salinity plots in Figure 2. Profiles for Hg speciation typically covered the upper water column to 200 m. BBL stations are locations where the continental shelf drops off and can have high levels of suspended sediments within the water column.[37] Samples at BBL stations were taken at one depth around 40−70 m identified as 5 m above the sea floor.[37]

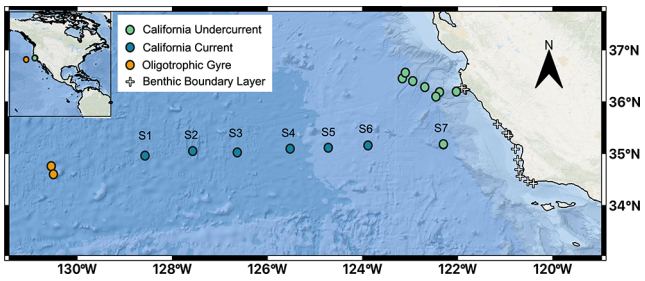

Figure 1. Sampling sites from the 2021 California Current Ecosystem Long-Term Ecological Research Process Cruise. Profiles are marked according to water mass for the California Undercurrent (green), California Current (blue), oligotrophic gyre (orange), and benthic boundary layer (BBL) (white crosses).

Sampling Methods. Vertical dissolved Hg profiles were sampled using 5 L X-Niskin bottles (Ocean Test Equipment) mounted on a trace metal rosette (Seabird) deployed on a nonmetallic hydroline[38,39] and triggered automatically by pressure on upcasts using a Seabird Auto Fire Module. BBL samples were collected using a 30 L Teflon-coated GO-Flo bottle (General Oceanics) deployed on a nonmetallic hydroline and triggered with an acid-cleaned Teflon messenger.[40] The Niskin or GO-Flo bottles were transported into a dedicated Class 100 laboratory van under trace metal-clean conditions.[39] Samples were pressure-filtered (N_2 gas, 99.99%) directly from the Niskin or GO-Flo bottles through 0.2 μm capsule filters (Acropak 200, Pall Laboratory) into 2 L acid-cleaned Teflon bottles.

An aliquot of sample was transferred from the 2 L Teflon bottle into 0.25 L precleaned borosilicate glass bottles (I-Chem) for THg analysis and oxidized with 0.04% bromine monochloride at least 12 h prior to analysis.[41]

The remainder of the sample in the 2 L Teflon bottle was analyzed for gaseous Hg^0 and DMHg with a purge-and-trap method.[42,43] Samples were purged with Hg-free N_2 gas for 60 min at a rate of 0.5 L min^{-1}. Effluent gas was passed through a soda lime trap to remove water vapor and aerosols, then DMHg was concentrated onto a Carbotrap (graphitized carbon black, Sigma-Aldrich) matrix downstream of the soda lime trap, and Hg^0 was concentrated onto a gold trap downstream of the Carbotrap.[43,44] DMHg was thermally desorbed from the Carbotrap and quantified on board via gas chromatographic cold vapor atomic fluorescence spectrometry (GC−CVAFS) on a Tekran 2500.[42,45] The detection limit for DMHg was 2 fM. Hg^0 was quantified by dual gold amalgamation cold vapor atomic fluorescence spectroscopy (CVAFS) on a Tekran 2600 following thermal desorption from the gold trap.[43,46] The detection limit for Hg^0 was 40 fM (n = 14). Sample concentrations for DMHg and Hg^0 were determined by a calibration curve from a gaseous Hg^0 standard (Tekran 2505 Mercury Vapor Primary Calibration Unit).

Seawater purged of DMHg and Hg^0 was transferred into 0.25 L precleaned amber borosilicate glass bottles (I-Chem) for MMHg analysis, acidified with 1% sulfuric acid (Trace-Metal Grade, Fisher Scientific), stored at 4 °C, and analyzed at Scripps Institution of Oceanography within 2 months of collection.

THg samples were analyzed following U.S. EPA Method 1631 on board the ship.[41,44] Samples were reduced to Hg^0 with

https://doi.org/10.1021/acs.est.4c01112
Environ. Sci. Technol. 2024, 58, 10591−10600

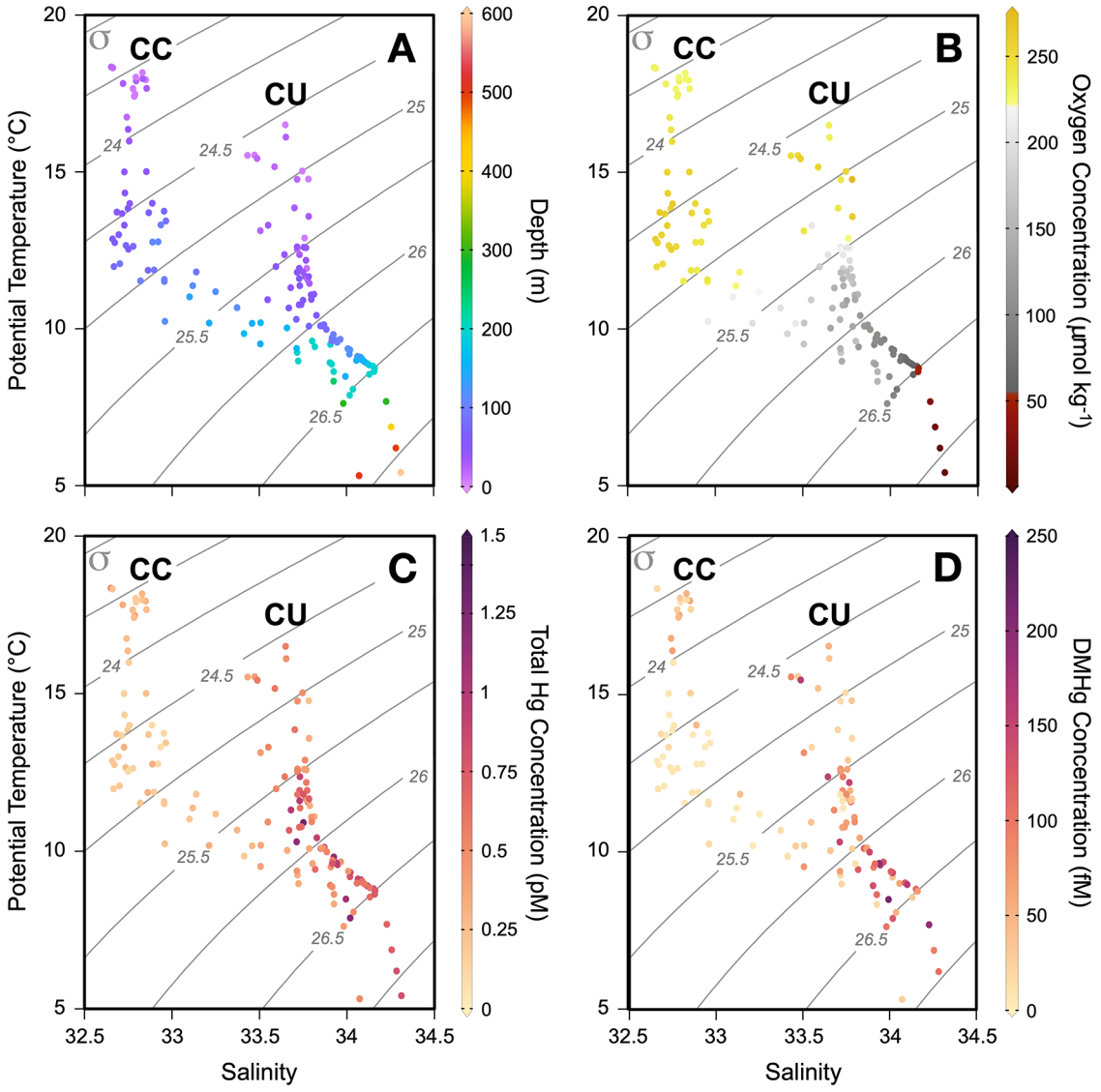

Figure 2. Temperature−salinity plots for (A) depth, (B) oxygen concentration, (C) dissolved total mercury (THg) concentration, and (D) dimethylmercury (DMHg) concentration. The curved gray lines indicate the isopycnals (σ). The California Current (CC) is on the left in lower salinities, and the California Undercurrent (CU) is on the right in higher salinities.

20% w/v tin(II) chloride solution (ACS grade, Fisher Chemical) in 10% hydrochloric acid (ACS grade, Fisher Chemical). Hg^0 was purged onto a gold trap with Hg-free argon gas and thermally desorbed via CVAFS for detection using a Tekran 2600 Automated Mercury Analyzer. Sample concentrations were determined by a calibration curve from a gaseous Hg^0 standard (Tekran 2505 Mercury Vapor Primary Calibration Unit). The detection limit was 0.22 pM (n = 8 reagent blanks), and the average replicate precision was 6.4% (n = 73).

MMHg samples were analyzed by ascorbic acid-assisted direct ethylation following Munson et al. and U.S. EPA Method 1630.[47,48] Samples were adjusted to a pH of 4.8 using a 2 M acetate/glacial acetic acid buffer (J.T. Baker) in ultrapure water (Milli-Q, 18.2 MΩ cm^{-1}) and 8 M potassium hydroxide (J.T. Baker) in ultrapure water (Milli-Q, 18.2 MΩ cm^{-1}). 2.5% w/v ascorbic acid (J.T. Baker) in ultrapure water (Milli-Q, 18.2 MΩ cm^{-1}) was added to the samples, and then samples were ethylated with sodium tetraethylborate (NaTEB) solution (1% NaTEB in 2% potassium hydroxide, Strem Chemicals) to convert MMHg to volatile methylethylmercury. Ethylation was allowed to proceed for 10 min before sample analysis. Samples were analyzed by GC−CVAFS on a Tekran 2700 Automated Methylmercury Analyzer. Concentrations were determined by a calibration curve from standards prepared from a certified 1000 ppm MMHg (II) chloride standard (Alfa Aesar). The detection limit was 11.3 fM (n = 9 reagent blanks), and ongoing precision and recovery was 98.4 ± 7.9% (n = 25). Average replicate precision was 9.2% (n = 18) and matrix spike recovery was 112 ± 13% (n = 15).

Auxiliary Parameters. Chl-*a* and dissolved organic carbon (DOC) were sampled from the standard CTD rosette cast that occurred just prior to the trace metal sampling and were analyzed using standard CCE LTER protocols (https://ccelter.ucsd.edu/cce-calcofi-methods-manual/).[49,50] Depth, temperature, salinity, and oxygen concentrations were determined from real-time hydrographic data from the ship's rosette (Seabird Scientific, SBE11, SBE-43, and SBE-45). These parameters are presented in Supplemental Table S1.

https://doi.org/10.1021/acs.est.4c01112
Environ. Sci. Technol. 2024, 58, 10591−10600

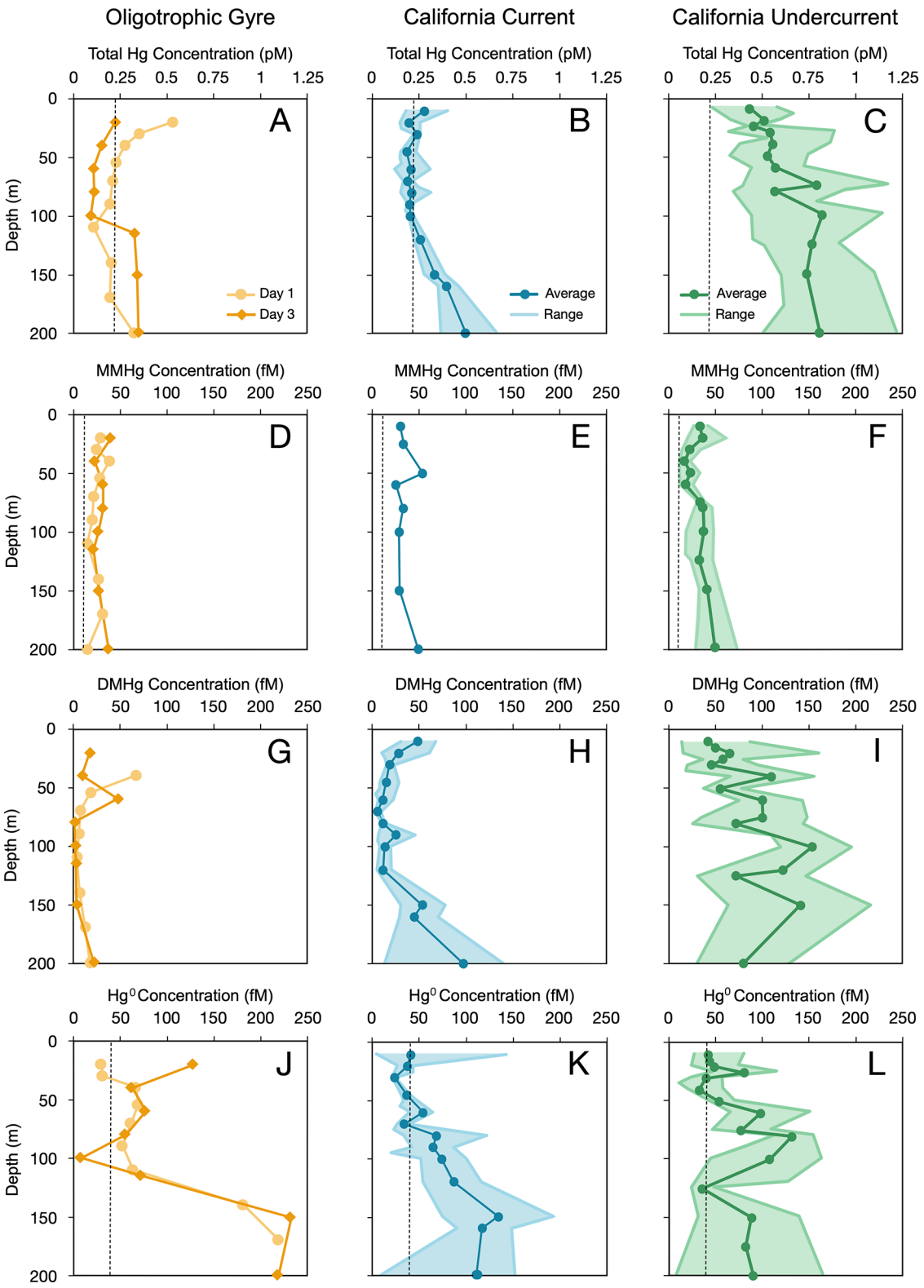

Figure 3. Profiles of dissolved Hg species for the (A, D, G, J) oligotrophic gyre, (B, E, H,K) California Current, and (C, F, I, L) the California Undercurrent. For the California Current and California Undercurrent, the average concentration of multiple profiles at each depth is plotted as the dark line, and the range is the shaded area. Detection limits are represented as the black dashed line as (A−C) 0.22 pM for total mercury (Hg), (D−F) 11.3 fM for monomethylmercury (MMHg), (G−I) 2 fM for dimethylmercury (DMHg), and (J−L) 40 fM for elemental mercury (Hg^0).

Wind speed was determined by an ultrasonic anemometer mounted on the ship's mast (RM Young, Model 86106).

Data Analysis. Data outliers for THg, MMHg, DMHg, and Hg^0 concentrations were identified using box and whisker plots, and values greater than 1.5 times the interquartile range above the third quartile were removed (Supplemental Figures S1 and S2). Of the 541 data points, we elected to remove 13 (<3%) statistical outliers that clearly stood out in the profiles.

https://doi.org/10.1021/acs.est.4c01112
Environ. Sci. Technol. 2024, 58, 10591−10600

Table 1. Mean ±1 Standard Deviation (SD) and Range of Concentrations of Dissolved Total Mercury (THg), Monomethylmercury (MMHg), Dimethylmercury (DMHg), and Elemental Mercury (Hg^0) throughout the Upper 200 m in the Study[a]

	THg (pM) mean ±1 SD (range)	MMHg (fM) mean ±1 SD (range)	DMHg (fM) mean ±1 SD (range)	Hg^0 (fM) mean ±1 SD (range)
California Undercurrent	0.64 ± 0.22 (0.24−1.21)	32.2 ± 13.9 (11.3−73.5)	84.0 ± 51.9 (14.5−215.3)	71.1 ± 42.2 (BDL − 161.8)
California Current	0.27 ± 0.12 (BDL − 0.67)	35.6 ± 10.5 (25.7−53.9)	29.5 ± 33.4 (2.3−137.6)	65.4 ± 45.9 (BDL − 193.9)
Oligotrophic gyre	0.25 ± 0.12 (BDL − 0.53)	28.1 ± 8.2 (14.5−45.8)	15.0 ± 18.6 (BDL − 66.8)	101.6 ± 73.2 (BDL − 230.8)
Benthic boundary layer	0.79 ± 0.23 (0.53−1.30)	44.5 ± 19.4 (16.8−75.6)	50.0 ± 30.6 (5.4−83.9)	53.5 ± 27.3 (BDL − 95.4)
All data	0.48 ± 0.27 (BDL − 1.30)	33.8 ± 14.9 (11.3−75.6)	56.5 ± 50.9 (2.3−215.3)	72.5 ± 48.6 (BDL − 230.8)

[a]BDL is the measured concentration below our detection limit. Concentrations are consistent with other measurements in the CCS and Pacific Ocean.[5,8,13,55] See Supplemental Table S1 for the calculated percent total methylated mercury values.

Individual daily profiles are presented in Supplemental Figure S3. To determine the statistical significance of relationships, we used one-way ANOVA and F-tests with $p = 0.05$ (Microsoft Excel Analysis ToolPak).

Mass Budget Model. We developed an empirically constrained mass budget model for the study region between the coast and Station S1 between 34°N and 37°N for the upper 200 m of the water column in MATLAB (Version R2022a). Processes in the model include (1) atmospheric deposition of Hg^{II} and MMHg and upwelling inputs of all Hg species, (2) exchange of all Hg species with surrounding seawater, (3) Hg^0 and DMHg air−sea interactions, (4) chemical transformations through Hg^0 and Hg^{II} redox reactions, Hg^{II} methylation to MMHg and DMHg, MMHg methylation to DMHg, MMHg demethylation to Hg^{II}, and DMHg demethylation to MMHg, and (5) scavenging of Hg^{II} and MMHg. We calculated reservoirs for each Hg species using depth-integrated averages of the data in this study, including the BBL samples. The conversions between Hg species were based on published rates from the literature. Our calculated DMHg demethylation rate (presented in the Results and Discussion section) was incorporated into this model. Atmospheric inputs were determined from literature values, while upwelling inputs were determined from depths between 300 and 600 m from one station in the California Undercurrent. Hg^{II} and MMHg removal from scavenging was determined from our solids budget (Figure S4) and suspended and sinking particle data published in Cui et al. (*Preprint*).[51] Hg^0 and DMHg, as dissolved gases, were not assumed to be present in the particulate phase. Evasion fluxes were calculated from ship-board wind speeds and upper water column profiles, and the outflow was based on the hydrology budget (Figure S4). Mass budgets for Hg^0, Hg^{II}, MMHg, and DMHg were used to create a set of coupled first-order differential equations to simulate changes in speciation over time.[34,52,53] See Supplemental Figures S4 and S5, Tables S2−S10, and eqs S1−S11 for more information.

We ran the model to steady state with a 12-h time step using averages of published Hg^{II} methylation and MMHg demethylation rates (Supplemental Table S10 and Supplemental Figures S6 and S7) along with the average upwelling speed determined by the Coastal Upwelling Transport Index (CUTI)[54] for July 2021. To evaluate variability in Hg^{II} methylation, MMHg demethylation, and upwelling speeds, we created a Monte Carlo simulation with 1000 iterations that randomly selected Hg^{II} methylation and MMHg demethylation rates within the 95% confidence interval of published values (Supplemental Table S10). For each combination of rates, we ran the model to steady state with varying upwelling speeds from 0 to 2 m d^{-1}, within the range of CUTI values for 2021.

RESULTS AND DISCUSSION

Distinct Water Mass THg Concentrations due to Scavenging in the California Undercurrent. The southern CCS has two dominant water masses: an oligotrophic water mass called the California Current and a more eutrophic water mass known as the California Undercurrent (Figure 1). The California Undercurrent is a narrow poleward-flowing current that is the principal source of upwelled waters in the region.[6] These are cold, higher salinity, nutrient-rich waters that stimulate biological productivity once upwelled[3] and are depleted in oxygen at depths greater than 100 m due to elevated particle formation and subsequent remineralization (Figure 2).[23,24] The upwelled waters form a surface water parcel that then advects offshore to the California Current in 40−80 days.[7] The California Current is an offshore surface current with an equatorward flow of warm, low salinity waters, and higher dissolved oxygen concentrations (Figure 2).[23] Figure 2C, 2D illustrate clear differences in THg and DMHg concentrations between the two water masses, and Figure 3 shows the upper water column profiles of all of the Hg species in each water mass. We find that the California Current has an average profile THg concentration 59% lower than the California Undercurrent ($p < 0.05$; Table 1, Figure 2C). These differences stem from the influence of upwelling transporting Hg-enriched deep waters to the surface of the California Undercurrent and then loss during water mass advection to the California Current.

Greater biological activity in upwelled nutrient-rich waters leads to increased particle production and sinking within the California Undercurrent.[3,23,24] The biological particle flux removes dissolved THg through scavenging and could explain the difference in THg concentrations between the California Undercurrent and the California Current. Using ship-board wind speeds, surface Hg^0 and DMHg concentrations, suspended and sinking particle THg concentrations,[51] and published air Hg^0 and DMHg concentrations,[56,57] we calculate that 123 pmol m^{-2} d^{-1} of Hg evades and 1621 pmol m^{-2} d^{-1} scavenges as the upwelled waters advect offshore and merge with the California Current (eqs S1−S9). Accounting for these removal processes, we calculate that it takes 47 ± 4 days for the dissolved THg concentrations in the upwelled water parcel to match those in the California Current (Supplemental Figure S8, eqs S12 and S13, Table S11). Because this time scale is consistent with the upwelled water parcel travel time of 40−80 days determined by Lagrangian particle trajectory analysis,[7] we conclude that scavenging can explain the majority of the

https://doi.org/10.1021/acs.est.4c01112
Environ. Sci. Technol. 2024, 58, 10591−10600

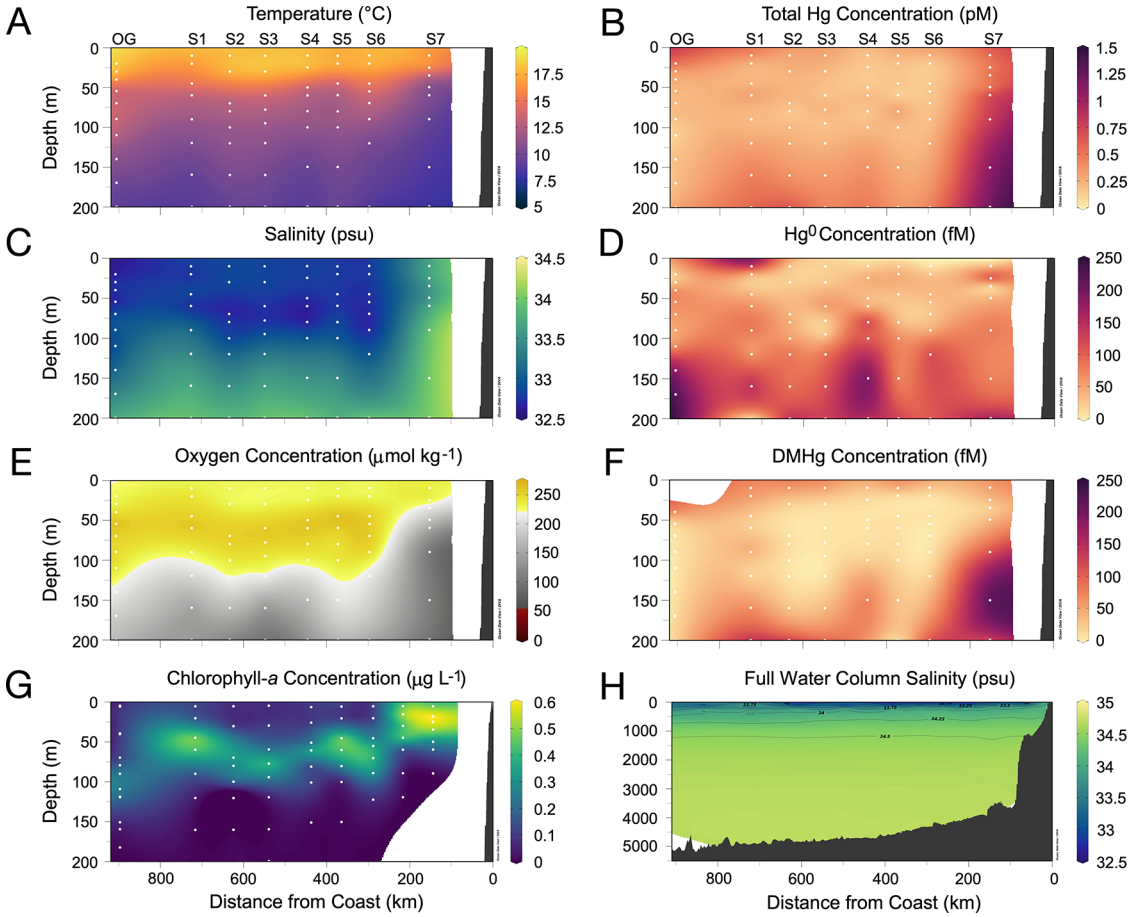

Figure 4. Section plots for the 7-station transect, including a profile from the oligotrophic gyre (OG) water mass. (A) Temperature, (B) total mercury (THg) concentration, (C) salinity, (D) elemental mercury (Hg^0) concentration, (E) oxygen concentration, (F) dimethylmercury (DMHg) concentration, (G) Chlorophyll-*a* concentration, and (H) full water column salinity with bathymetry from the World Ocean Circulation Experiment (WOCE).[59]

difference in THg concentrations observed between the two water masses.

The cycle of upwelling, scavenging, and particle remineralization traps most of the THg within the highly productive California Undercurrent. Figure 4 illustrates this with the sharp difference between Stations S6 and S7 where the two water masses meet, demonstrating that most of these losses occur within 200 km of the coast. These dynamics have also been observed in the Peruvian Upwelling System, where upwelling increases surface THg concentrations close to the coast that do not persist offshore.[13] One explanation is that increased scavenging and remineralization results in increased rates of Hg accumulation within sediment cores, which is correlated with marine productivity.[58] In these systems, elevated THg concentrations are sustained within the source waters for upwelling, and due to the elevated productivity in the region, we hypothesize that these upwelling regions are a prime location for Hg incorporation into food webs.

DMHg Is Upwelled to Surface Waters in the California Undercurrent and Demethylates During Water Parcel Advection. Little is known about the formation of DMHg in the ocean; however, it has been found in high concentrations in suboxic (<50 μmol kg^{-1}) conditions.[4,5,13,14] Here, we find an inverse relationship between DMHg and oxygen concentrations (R^2 = 0.42, n = 121, p < 0.05, Supplemental Figure S9), which suggests that the low oxygen concentrations present in the California Undercurrent favor DMHg formation or preservation (Figure 2B). Below 200 m, the California Undercurrent is further depleted in oxygen (<50 μmol kg^{-1}),[23] implying that DMHg concentrations could be considerably higher at depth. Once upwelled, the low oxygen and high DMHg deeper waters are diluted by oxic and low DMHg surface waters that are subject to losses from photodemethylation and evasion. These processes inhibit DMHg accumulation in the majority of the global surface ocean.[5,25] Within the surface water masses that we studied, we find that the California Undercurrent contains 69% higher DMHg concentrations than the California Current (p < 0.05, Figure 2D). We attribute this difference to the continuous supply of DMHg to surface waters from the upwelling of DMHg-enriched deeper waters in the California Undercurrent. Then, during surface advection to the California Current, DMHg evades to the atmosphere or demethylates into MMHg, which explains depleted concentrations in the California Current.

We calculated in the previous section that dissolved THg removal in the advecting water parcel takes 47 ± 4 days, and we apply this transit time to calculate DMHg removal due to evasion and demethylation. We estimate evasion losses of 96 ± 16 pmol m^{-2} d^{-1} using ship-board wind speeds, average surface DMHg concentration, and published air DMHg concentration[56] (Supplemental eqs S1−S9, Table S6). Assuming no

https://doi.org/10.1021/acs.est.4c01112
Environ. Sci. Technol. 2024, 58, 10591−10600

settling or other inputs of DMHg, we calculate a net DMHg demethylation rate of 2.0 ± 1.1% d^{-1} that is needed to close the DMHg budget (Supplemental Figure S10, eqs S14−S17, and Table S12). This approach allows us to estimate a region-specific dark and photolytic DMHg degradation rate. Estimates of photodemethylation exist; for example, West et al. reported a rate of 0.15 ± 0.01% d^{-1} (when corrected for shortwave radiation exposure; Supplemental eq S18, Table S13).[25] However, dark DMHg demethylation rates are unknown and could range from 0.003 to 44% d^{-1} if DMHg behaves like MMHg.[15,20,26−31] Thus, our approach constrains the DMHg demethylation rate in the CCS before applying it to a mass budget model to evaluate how this process impacts the supply of MMHg.

DMHg Demethylation Is a Substantial Source of Surface MMHg in Upwelling Conditions. In contrast to THg and DMHg concentrations, dissolved MMHg concentrations are the same in the California Undercurrent and the California Current ($p > 0.05$, Table 1, Figure 3). As the water parcel moves from the California Undercurrent, we would expect MMHg losses from scavenging,[51] photodemethylation,[25] and dark demethylation.[15,20,26−31] The lack of apparent change in MMHg concentrations between the water masses suggests a resupply of MMHg through atmospheric deposition, upwelling, Hg^{II} methylation, or DMHg demethylation. To quantify the relative contribution of each source of MMHg to surface waters, we developed an empirically constrained mass budget model that encompasses both the productive California Undercurrent and the oligotrophic California Current.

Figure 5A presents the mass budget incorporating our calculated DMHg demethylation rate to visualize the transformations between the Hg species. Net DMHg demethylation and upwelling are the two largest inputs of MMHg contributing, respectively, 2.3 and 1.3 mol d^{-1}. Photodemethylation and net MMHg demethylation to Hg^{II} remove 1.5 and 1.7 mol d^{-1} of MMHg, respectively. We find that within these surface waters, net DMHg demethylation is a source of MMHg while there is no net source of MMHg from Hg^{II} methylation. As a result, DMHg degradation is the major source of MMHg, accounting for 61% of the MMHg supply.

Using this model, we can evaluate the relative importance of the processes impacting Hg speciation within the system. Hg^{II} methylation is typically considered to be the main source of MMHg, while DMHg demethylation is overlooked. Figure 5B presents the mass budget of the system without demethylation of DMHg into MMHg. In this scenario, the main source of MMHg is from net Hg^{II} methylation, at a rate of 1.3 mol d^{-1}. Without DMHg demethylation, the balance between Hg species is shifted and requires net Hg^{II} methylation, which is unlikely to occur in oxygenated and illuminated surface waters. On the other hand, DMHg demethylation can supply enough MMHg to sustain net MMHg demethylation.[25]

The literature is unclear whether DMHg is formed from MMHg, Hg^{II}, or both. Field incubations from Lehnherr et al. showed DMHg formation from MMHg and Hg^{II},[21] whereas a laboratory study indicated that DMHg forms from MMHg but not Hg^{II}.[22] Figure S11 shows that removing the Hg^{II} to DMHg methylation pathway results in less than a 10% decrease in the transformation rates between Hg species and does not impact the reservoir sizes. Because of this lack of significant impact, we chose the conservative approach and included DMHg formation from MMHg and Hg^{II} in our model.

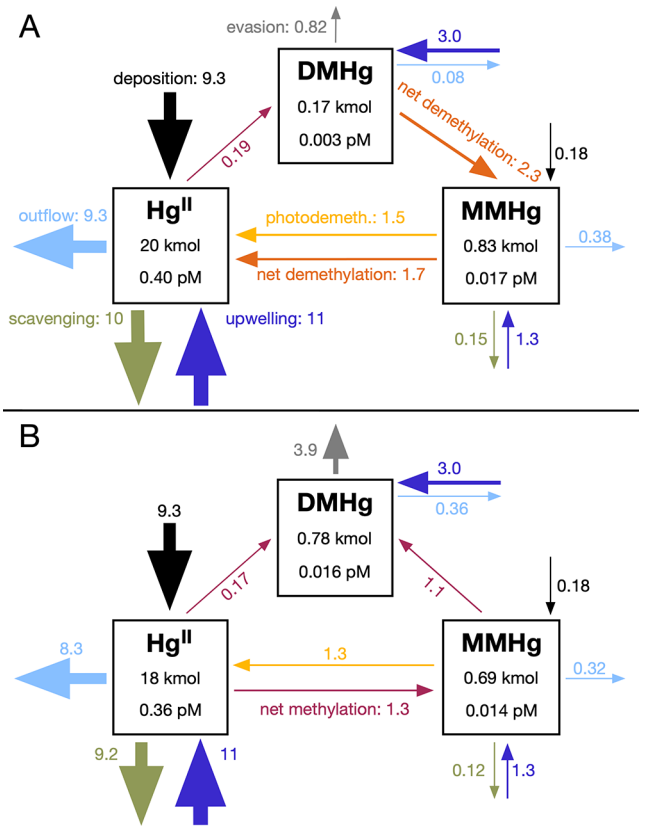

Figure 5. Steady-state mass budget (A) with DMHg demethylation and (B) without DMHg demethylation. Rates represented by the arrows are given in mol d^{-1}. Hg^0 reservoir, fluxes, and redox reactions are included in the model but not pictured here. Arrows are scaled to the magnitude of the rates, and each process is represented by a different color.

In the initial model run, we set the DMHg demethylation rate to 2.0% d^{-1} based on our calculations and used averages for the Hg^{II} methylation rate (0.25% d^{-1}), MMHg demethylation rate (6.2% d^{-1}), and upwelling speed for July 2021 (0.9 m d^{-1}).[54] These rates account for most of the variability in model outputs for MMHg concentrations, sources, and sinks based on our model sensitivity analysis. Hg^{II} methylation and MMHg demethylation rates are based on published values and cover wide ranges of sampling locations and conditions; 0.007−5.17% d^{-1} for Hg^{II} methylation[15,19−21,26−31] and 0.003−44% for MMHg demethylation (Supplemental Table S10).[15,20,26−31] Another source of large variability in the model is the upwelling speed, as it is seasonally driven by wind speeds, with average monthly upwelling speeds ranging from 0.2 to 2.0 m d^{-1} in 2021.[54] Finally, our calculated DMHg demethylation rates range from 0.9 to 3.1% d^{-1}. To test the validity of our main finding that upwelled DMHg demethylation is the major source of MMHg in surface waters in the CCS in the context of these large uncertainties, we ran the model while changing DMHg and MMHg demethylation and Hg^{II} methylation rates.

Figure 6A shows the sources of MMHg as the DMHg demethylation rate increases from 0 to 3% d^{-1}. We see that with a rate as low as 0.4% d^{-1}, net DMHg demethylation still accounts for 30% of the MMHg in the system. Net Hg^{II} methylation is only a source of MMHg in the system when the DMHg demethylation rate is between 0 and 0.3% d^{-1}. DMHg

https://doi.org/10.1021/acs.est.4c01112
Environ. Sci. Technol. 2024, 58, 10591−10600

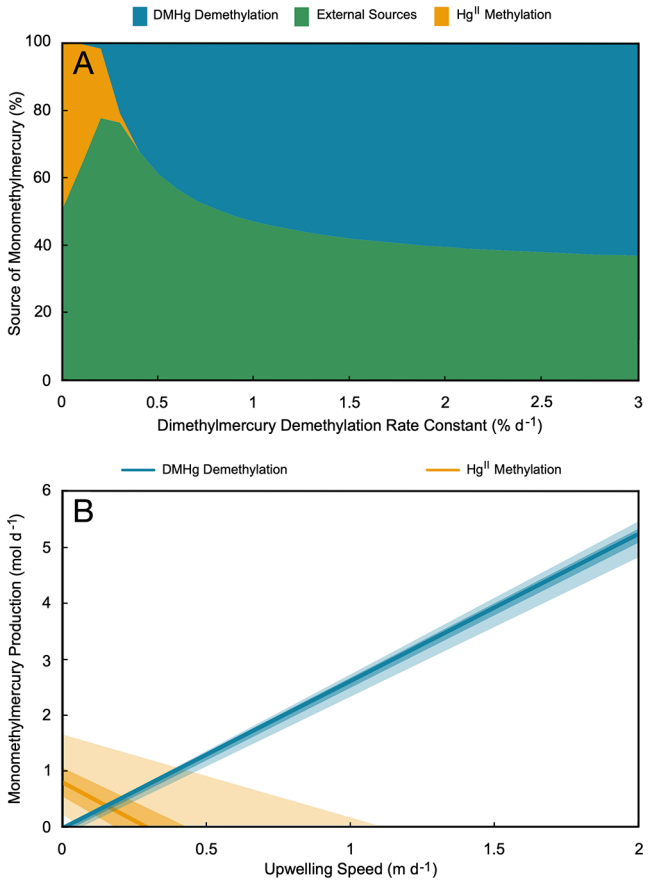

Figure 6. (A) Sources of monomethylmercury (MMHg) as dimethylmercury (DMHg) demethylation rate increases. External sources (green) include upwelling and direct deposition. DMHg demethylation (blue) and Hg^{II} methylation (orange) represent the net production of MMHg from those reactions. (B) Monomethylmercury production from net Hg^{II} methylation (orange) and net DMHg demethylation (blue) as the upwelling speed increases. The line represents the median of 1000 simulations with the dark shaded area representing the region between the 25th and 75th quartiles and the light shaded area representing 1.5 times the interquartile range.

exceeds 50% of the source of MMHg when the DMHg demethylation rate is 0.9% d^{-1}. This supports the idea that DMHg represents a substantial source of MMHg across a wide range of DMHg demethylation rates.

To assess the impact of varying Hg^{II} methylation and MMHg demethylation rates reported in the literature, we ran the model 1000 times with different upwelling speeds. During each iteration, the model randomly selected rates within the 95% confidence interval of published values. Figure 6B shows the modeled net MMHg production from Hg^{II} methylation (orange) and DMHg degradation (blue) plotted against the upwelling speeds. Without upwelling, the model shows a median MMHg production rate of 0.8 mol d^{-1} from Hg^{II} methylation alone. However, the model likely overestimates MMHg production in these surficial waters because we use rates from deeper waters and from studies that did not differentiate between MMHg and DMHg formation. Thus, we expect very low to no MMHg production in the absence of upwelling. During upwelling events, under the most likely rates (dark shading), net DMHg demethylation surpasses the average contribution of MMHg from net Hg^{II} methylation at an upwelling speed of roughly 0.2 m d^{-1}. With the least likely Hg^{II} methylation and MMHg degradation rates (light shading), net DMHg demethylation again delivers most of the MMHg to the system above an upwelling speed of 0.4 m d^{-1}, which is common throughout the year. Therefore, we conclude that in the CCS and possibly other locations where upwelling supplies DMHg to surface water, DMHg demethylation rather than Hg^{II} methylation is the main source of MMHg to the epipelagic zone.

■ ASSOCIATED CONTENT

Supporting Information

The Supporting Information is available free of charge at https://pubs.acs.org/doi/10.1021/acs.est.4c01112.

Additional hydrological parameters (Table S1) data analysis details (box and whisker plots, Figures S1 and S2), individual mercury species profiles (Figure S3), empirical mass budget model parameters (Figures S4−S7, Table S2−S10, Equation S1−S11), and calculations (Figures S8−S11, Tables S11−S13, and Equations S12−S18) (PDF)

■ AUTHOR INFORMATION

Corresponding Authors

Hannah M. Adams − *Scripps Institution of Oceanography, University of California San Diego, La Jolla, California 92037, United States;* orcid.org/0000-0001-7231-3522; Email: hadams@ucsd.edu

Amina T. Schartup − *Scripps Institution of Oceanography, University of California San Diego, La Jolla, California 92037, United States;* orcid.org/0000-0002-9289-8107; Email: aschartup@ucsd.edu

Authors

Xinyun Cui − *Ocean Sciences Department, University of California Santa Cruz, Santa Cruz, California 95064, United States;* orcid.org/0009-0005-6331-6226

Carl H. Lamborg − *Ocean Sciences Department, University of California Santa Cruz, Santa Cruz, California 95064, United States*

Complete contact information is available at: https://pubs.acs.org/10.1021/acs.est.4c01112

Notes

The authors declare no competing financial interest.

■ ACKNOWLEDGMENTS

We thank the captains and crews of the CCE LTER P2107 cruise (RR2105) as well as the scientific crews who collected the samples. We acknowledge the U.S. National Science Foundation (grant #OCE-2023046 to A.T.S. and C.H.L. and grant #OCE-1637632 to the CCE LTER Program) that supported the collection, analysis, and writing of this current work. We thank J. West, C. Sephus, E. Paulson, I. Kübler-Dudgeon, R. Ovbiebo, K. Barbeau, J. Bowman, and J. Figueroa for their review and feedback to this manuscript. A.T.S. and C.H.L. conceived of the presented idea and designed the study. H.M.A., X.C., C.H.L., and A.T.S. collected Hg data sets. H.M.A. and A.T.S. performed the data analysis and modeling and drafted the manuscript. All authors contributed to editing the manuscript.

REFERENCES

(1) Sunderland, E. M. Mercury Exposure from Domestic and Imported Estuarine and Marine Fish in the U.S. Seafood Market. *Environ. Health Perspect* **2007**, *115* (2), 235−242.

(2) National Oceanic & Atmospheric Administration. California Current Region. National Marine Ecosystem Status. https://ecowatch.noaa.gov/regions/california-current (accessed July 31, 2022).

(3) Rykaczewski, R. R.; Checkley, D. M.; Davis, R. E. Influence of Ocean Winds on the Pelagic Ecosystem in Upwelling Regions. *Proc. Natl. Acad. Sci.* **2008**, *105* (6), 1965−1970.

(4) Conaway, C. H.; Black, F. J.; Gault-Ringold, M.; Pennington, J. T.; Chavez, F. P.; Flegal, A. R. Dimethylmercury in Coastal Upwelling Waters, Monterey Bay, California. *Environ. Sci. Technol.* **2009**, *43* (5), 1305−1309.

(5) Coale, K. H.; Heim, W. A.; Negrey, J.; Weiss-Penzias, P.; Fernandez, D.; Olson, A.; Chiswell, H.; Byington, A.; Bonnema, A.; Martenuk, S.; Newman, A.; Beebe, C.; Till, C. The Distribution and Speciation of Mercury in the California Current: Implications for Mercury Transport via Fog to Land. *Deep Sea Res. 2 Top Stud Oceanogr.* **2018**, *151* (May), 77−88.

(6) Zaba, K. D.; Franks, P. J. S.; Ohman, M. D. The California Undercurrent as a Source of Upwelled Waters in a Coastal Filament. *J. Geophys Res. Oceans* **2021**, *126* (2), e2020JC016602 DOI: 10.1029/2020JC016602.

(7) Chabert, P.; d'Ovidio, F.; Echevin, V.; Stukel, M. R.; Ohman, M. D. Cross-Shore Flow and Implications for Carbon Export in the California Current Ecosystem: A Lagrangian Analysis. *J. Geophys Res. Oceans* **2021**, *126* (2), e2020JC016611 DOI: 10.1029/2020JC016611.

(8) Laurier, F. J. G.; Mason, R. P.; Gill, G. A.; Whalin, L. Mercury Distributions in the North Pacific Ocean - 20 Years of Observations. *Marine Chem.* **2004**, *90*, 3−19.

(9) Mason, R. P.; Fitzgerald, W. F.; Morel, F. M. M. The Biogeochemical Cycling of Elemental Mercury: Anthropogenic Influences. *Geochim. Cosmochim. Acta* **1994**, *58* (15), 3191−3198.

(10) Benoit, J. M.; Gilmour, C. C.; Mason, R. P.; Heyes, A. Sulfide Controls on Mercury Speciation and Bioavailability to Methylating Bacteria in Sediment Pore Waters. *Environ. Sci. Technol.* **1999**, *33* (6), 951−957.

(11) Compeau, G.; Bartha, R. Methylation and Demethylation of Mercury under Controlled Redox, PH, and Salinity Conditions. *Appl. Environ. Microbiol.* **1984**, *48* (6), 1203−1207.

(12) Bowman, K. L.; Hammerschmidt, C. R.; Lamborg, C. H.; Swarr, G. Mercury in the North Atlantic Ocean: The U.S. GEOTRACES Zonal and Meridional Sections. *Deep Sea Res. 2 Top Stud Oceanogr.* **2015**, *116*, 251−261.

(13) Bowman, K. L.; Hammerschmidt, C. R.; Lamborg, C. H.; Swarr, G. J.; Agather, A. M. Distribution of Mercury Species across a Zonal Section of the Eastern Tropical South Pacific Ocean (U.S. GEOTRACES GP16). *Mar. Chem.* **2016**, *186*, 156−166.

(14) Mason, R. P.; Fitzgerald, W. F. Alkylmercury Species in the Equatorial Pacific. *Nature* **1990**, *347* (1990), 457−459.

(15) Soerensen, A. L.; Schartup, A. T.; Skrobonja, A.; Bouchet, S.; Amouroux, D.; Liem-Nguyen, V.; Björn, E. Deciphering the Role of Water Column Redoxclines on Methylmercury Cycling Using Speciation Modeling and Observations From the Baltic Sea. *Global Biogeochem. Cycles* **2018**, *32* (10), 1498−1513.

(16) Parks, J. M.; Johs, A.; Podar, M.; Bridou, R.; Hurt, R. A.; Smith, S. D.; Tomanicek, S. J.; Qian, Y.; Brown, S. D.; Brandt, C. C.; Palumbo, A. v.; Smith, J. C.; Wall, J. D.; Elias, D. A.; Liang, L. The Genetic Basis for Bacterial Mercury Methylation. *Science* **2013**, *339* (6125), 1332−1335.

(17) Gilmour, C. C.; Elias, D. A.; Kucken, A. M.; Brown, S. D.; Palumbo, A. V.; Schadt, C. W.; Wall, J. D. Sulfate-Reducing Bacterium Desulfovibrio Desulfuricans ND132 as a Model for Understanding Bacterial Mercury Methylation. *Appl. Environ. Microbiol.* **2011**, *77* (12), 3938−3951.

(18) Bowman, K. L.; Collins, R. E.; Agather, A. M.; Lamborg, C. H.; Hammerschmidt, C. R.; Kaul, D.; Dupont, C. L.; Christensen, G. A.; Elias, D. A. Distribution of Mercury-Cycling Genes in the Arctic and Equatorial Pacific Oceans and Their Relationship to Mercury Speciation. *Limnol. Oceanogr.* **2020**, *65* (S1), S310−S320.

(19) Despins, M. C.; Mason, R. P.; Aguilar-Islas, A. M.; Lamborg, C. H.; Hammerschmidt, C. R.; Newell, S. E. Linked Mercury Methylation and Nitrification across Oxic Subpolar Regions. *Front. Environ. Chem.* **2023**, *4*, 1109537 DOI: 10.3389/fenvc.2023.1109537.

(20) Capo, E.; Feng, C.; Bravo, A. G.; Bertilsson, S.; Soerensen, A. L.; Pinhassi, J.; Buck, M.; Karlsson, C.; Hawkes, J.; Björn, E. Expression Levels of HgcAB Genes and Mercury Availability Jointly Explain Methylmercury Formation in Stratified Brackish Waters. *Environ. Sci. Technol.* **2022**, *56* (18), 13119−13130.

(21) Lehnherr, I.; St Louis, V. L.; Hintelmann, H.; Kirk, J. L. Methylation of Inorganic Mercury in Polar Marine Waters. *Nat. Geosci* **2011**, *4* (5), 298−302.

(22) Jonsson, S.; Mazrui, N. M.; Mason, R. P. Dimethylmercury Formation Mediated by Inorganic and Organic Reduced Sulfur Surfaces. *Sci. Rep* **2016**, *6*, No. 27958.

(23) Checkley, D. M.; Barth, J. A. Patterns and Processes in the California Current System. *Prog. Oceanogr.* **2009**, *83* (1−4), 49−64.

(24) Stukel, M. R.; Aluwihare, L. I.; Barbeau, K. A.; Chekalyuk, A. M.; Goericke, R.; Miller, A. J.; Ohman, M. D.; Ruacho, A.; Song, H.; Stephens, B. M.; Landry, M. R. Mesoscale Ocean Fronts Enhance Carbon Export Due to Gravitational Sinking and Subduction. *Proc. Natl. Acad. Sci. U.S.A.* **2017**, *114* (6), 1252−1257.

(25) West, J.; Gindorf, S.; Jonsson, S. Photochemical Degradation of Dimethylmercury in Natural Waters. *Environ. Sci. Technol.* **2022**, *56* (9), 5920−5928.

(26) Monperrus, M.; Tessier, E.; Amouroux, D.; Leynaert, A.; Huonnic, P.; Donard, O. F. X. Mercury Methylation, Demethylation and Reduction Rates in Coastal and Marine Surface Waters of the Mediterranean Sea. *Mar Chem.* **2007**, *107* (1), 49−63.

(27) Munson, K. M.; Lamborg, C. H.; Boiteau, R. M.; Saito, M. A. Dynamic Mercury Methylation and Demethylation in Oligotrophic Marine Water. *Biogeosciences* **2018**, *15* (21), 6451−6460.

(28) Munson, K. M. *Transformations of Mercury in the Marine Water Column*; Massachusetts Institute of Technology and Woods Hole Oceanographic Institution, Boston, MA, 2014.

(29) Sharif, A.; Monperrus, M.; Tessier, E.; Bouchet, S.; Pinaly, H.; Rodriguez-Gonzalez, P.; Maron, P.; Amouroux, D. Fate of Mercury Species in the Coastal Plume of the Adour River Estuary (Bay of Biscay, SW France). *Sci. Total Environ.* **2014**, *496*, 701−713.

(30) Bouchet, S.; Amouroux, D.; Rodriguez-Gonzalez, P.; Tessier, E.; Monperrus, M.; Thouzeau, G.; Clavier, J.; Amice, E.; Deborde, J.; Bujan, S.; Grall, J.; Anschutz, P. MMHg Production and Export from Intertidal Sediments to the Water Column of a Tidal Lagoon (Arcachon Bay, France). *Biogeochemistry* **2013**, *114* (1−3), 341−358.

(31) Schartup, A. T.; Soerensen, A.; Calder, R.; Heimbürger-Boavida, L.-E. Vertical Distribution of Methylmercury in the Central Arctic Ocean Explained by In Situ Methylation and Demethylation *Environ. Sci. Technol.*, in review.

(32) West, J.; Graham, A. M.; Liem-Nguyen, V.; Jonsson, S. Dimethylmercury Degradation by Dissolved Sulfide and Mackinawite. *Environ. Sci. Technol.* **2020**, *54* (21), 13731−13738.

(33) Zhang, Y.; Soerensen, A. L.; Schartup, A. T.; Sunderland, E. M. A Global Model for Methylmercury Formation and Uptake at the Base of Marine Food Webs. *Global Biogeochem. Cycles* **2020**, *34* (2), e2019GB006348 DOI: 10.1029/2019GB006348.

(34) Soerensen, A. L.; Jacob, D. J.; Schartup, A. T.; Fisher, J. A.; Lehnherr, I., St; Louis, V. L.; Heimburger, L. E.; Sonke, J. E.; Krabbenhoft, D. P.; Sunderland, E. M. A Mass Budget for Mercury and Methylmercury in the Arctic Ocean. *Global Biogeochem. Cycles* **2016**, *30* (4), 560−575.

(35) Krause, J. W.; Brzezinski, M. A.; Goericke, R.; Landry, M. R.; Ohman, M. D.; Stukel, M. R.; Taylor, A. G. Variability in Diatom Contributions to Biomass, Organic Matter Production and Export

across a Frontal Gradient in the California Current Ecosystem. *J. Geophys Res. Oceans* **2015**, *120* (2), 1032−1047.
(36) Landry, M. R.; Ohman, M. D.; Goericke, R.; Stukel, M. R.; Tsyrklevich, K. Lagrangian Studies of Phytoplankton Growth and Grazing Relationships in a Coastal Upwelling Ecosystem off Southern California. *Prog. Oceanogr.* **2009**, *83* (1−4), 208−216.
(37) Biller, D. V.; Bruland, K. W. Sources and Distributions of Mn, Fe, Co, Ni, Cu, Zn, and Cd Relative to Macronutrients along the Central California Coast during the Spring and Summer Upwelling Season. *Mar. Chem.* **2013**, *155*, 50−70.
(38) Brzezinski, M. A.; Krause, J. W.; Bundy, R. M.; Barbeau, K. A.; Franks, P.; Goericke, R.; Landry, M. R.; Stukel, M. R. Enhanced Silica Ballasting from Iron Stress Sustains Carbon Export in a Frontal Zone within the California Current. *J. Geophys Res. Oceans* **2015**, *120* (7), 4654−4669.
(39) Cutter, G. A.; Bruland, K. W. Rapid and Noncontaminating Sampling System for Trace Elements in Global Ocean Surveys. *Limnol. Oceanogr. Methods* **2012**, *10*, 425−436.
(40) Bruland, K. W.; Franks, R. P.; Knauer, G. A.; Martin, J. H. Sampling and Analytical Methods for the Determination of Copper, Cadmium, Zinc, and Nickel at the Nanogram per Liter Level in Sea Water. *Anal. Chim. Acta* **1979**, *105*, 233−245.
(41) U.S. Environmental Protection Agency. *Method 1631, Revision E: Mercury in Water by Oxidation, Purge and Trap, and Cold Vapor Atomic Fluorescence Spectrometry Method 1631, Revision E: Mercury in Water by Oxidation, Purge and Trap, and Cold Vapor Atomic Fluorescence Spectrometry Method 1631, Revision E*; Washington, D.C., 2002.
(42) Bowman, K. L.; Hammerschmidt, C. R. Extraction of Monomethylmercury from Seawater for Low-Femtomolar Determination. *Limnol. Oceanogr. Methods* **2011**, *9*, 121−128.
(43) Tseng, C. M.; Lamborg, C.; Fitzgerald, W. F.; Engstrom, D. R. Cycling of Dissolved Elemental Mercury in Arctic Alaskan Lakes. *Geochim. Cosmochim. Acta* **2004**, *68* (6), 1173−1184.
(44) Lamborg, C. H.; Hammerschmidt, C. R.; Gill, G. A.; Mason, R. P.; Gichuki, S. An Intercomparison of Procedures for the Determination of Total Mercury in Seawater and Recommendations Regarding Mercury Speciation during GEOTRACES Cruises. *Limnol. Oceanogr. Methods* **2012**, *10*, 90−100.
(45) Baya, P. A.; Hollinsworth, J. L.; Hintelmann, H. Evaluation and Optimization of Solid Adsorbents for the Sampling of Gaseous Methylated Mercury Species. *Anal. Chim. Acta* **2013**, *786*, 61−69.
(46) Bloom, N.; Fitzgerald, W. F. Determination of Volatile Mercury Species at the Picogram Level by Low-Temperature Gas Chromatography with Cold-Vapour Atomic Fluorescence Detection. *Anal. Chim. Acta* **1988**, *208*, 151−161.
(47) U.S. Environmental Protection Agency. *Method 1630: Methyl Mercury in Water by Distillation, Aqueous Ethylation, Purge and Trap, and Cold Vapor Atomic Fluorescence Spectrometry* 1998.
(48) Munson, K. M.; Babi, D.; Lamborg, C. H. Determination of Monomethylmercury from Seawater with Ascorbic Acid-Assisted Direct Ethylation. *Limnol Oceanogr Methods* **2014**, *12*, 1−9.
(49) Goericke, R.; Stukel, M.; California Current Ecosystem LTER. Chlorophyll and phaeopigments measured from discrete bottle samples from CCE LTER process cruises in the California Current System, determined by extraction and bench fluorometry, 2006−2021 (ongoing). Environmental Data Initiative. https://portal.edirepository.org/nis/mapbrowse?packageid=knb-lter-cce.11.10.
(50) Aluwihare, L. California Current Ecosystem LTERTotal dissolved organic carbon and nitrogen measurements at selected depths in the water column from CCE LTER process cruises in the California Current System, 2006 - 2017 (ongoing). Environmental Data Initiative. https://portal.edirepository.org/nis/mapbrowse?packageid=knb-lter-cce.20.5.
(51) Cui, X.; Adams, H. M.; Schartup, A. T.; Song, Y.; Stukel, M.; Lamborg, C. H. *Upwelling Enhances Mercury Particle Scavenging in the California Current Ecosystem*. Submitted 2024−03−15. *Research Square*. DOI: 10.21203/rs.3.rs-4102885/v1 (accessed 2024−04−15).
(52) Schartup, A. T.; Balcom, P. H.; Soerensen, A. L.; Gosnell, K. J.; Calder, R. S. D.; Mason, R. P.; Sunderland, E. M.; Louis, V. L., St. Freshwater Discharges Drive High Levels of Methylmercury in Arctic Marine Biota. *Proc. Natl. Acad. Sci. U.S.A.* **2015**, *112* (38), 11789−11794.
(53) Sunderland, E. M.; Dalziel, J.; Heyes, A.; Branfireun, B. A.; Krabbenhoft, D. P.; Gobas, F. A. P. C. Response of a Macrotidal Estuary to Changes in Anthropogenic Mercury Loading between 1850 and 2000. *Environ. Sci. Technol.* **2010**, *44* (5), 1698−1704.
(54) Jacox, M. G.; Edwards, C. A.; Hazen, E. L.; Bograd, S. J. Coastal Upwelling Revisited: Ekman, Bakun, and Improved Upwelling Indices for the U.S. West Coast. *J. Geophys Res. Oceans* **2018**, *123* (10), 7332−7350.
(55) Sunderland, E. M.; Krabbenhoft, D. P.; Moreau, J. W.; Strode, S. A.; Landing, W. M. Mercury Sources, Distribution, and Bioavailability in the North Pacific Ocean: Insights from Data and Models. *Global Biogeochem Cycles* **2009**, *23*. DOI: 10.1029/2008GB003425.
(56) Baya, P. A.; Gosselin, M.; Lehnherr, I.; St Louis, V. L.; Hintelmann, H. Determination of Monomethylmercury and Dimethylmercury in the Arctic Marine Boundary Layer. *Environ. Sci. Technol.* **2015**, *49* (1), 223−232.
(57) Weiss-Penzias, P. S.; Williams, E. J.; Lerner, B. M.; Bates, T. S.; Gaston, C.; Prather, K.; Vlasenko, A.; Li, S. M. Shipboard Measurements of Gaseous Elemental Mercury along the Coast of Central and Southern California. *J. Geophys. Res. Atmospheres* **2013**, *118* (1), 208−219.
(58) Zaferani, S.; Biester, H. Mercury Accumulation in Marine Sediments − A Comparison of an Upwelling Area and Two Large River Mouths. *Front. Marine Sci.* **2021**, *8*, 732720 DOI: 10.3389/fmars.2021.732720.
(59) *The World Ocean Circulation Experiment (WOCE) Global Hydrographic Climatology*; Research Data Archive at the National Center for Atmospheric Research, Computational and Information Systems Laboratory.